

Concurrent Sign-off Timing Optimization via Deep Steiner Points Refinement

Siting Liu^{1,2†}, Ziyi Wang^{1†}, Fangzhou Liu¹,
Yibo Lin², Bei Yu¹, Martin Wong¹

¹Chinese University of Hong Kong, ²Peking University



Introduction

- Optimizing the sign-off metrics in early stages requires a full time-consuming physical design flow.
- Recent progress in machine learning (ML) has permitted fast and precise evaluation skipping a complex process.
- Early-stage timing optimization is critical for timing closure to reduce the turnaround time.

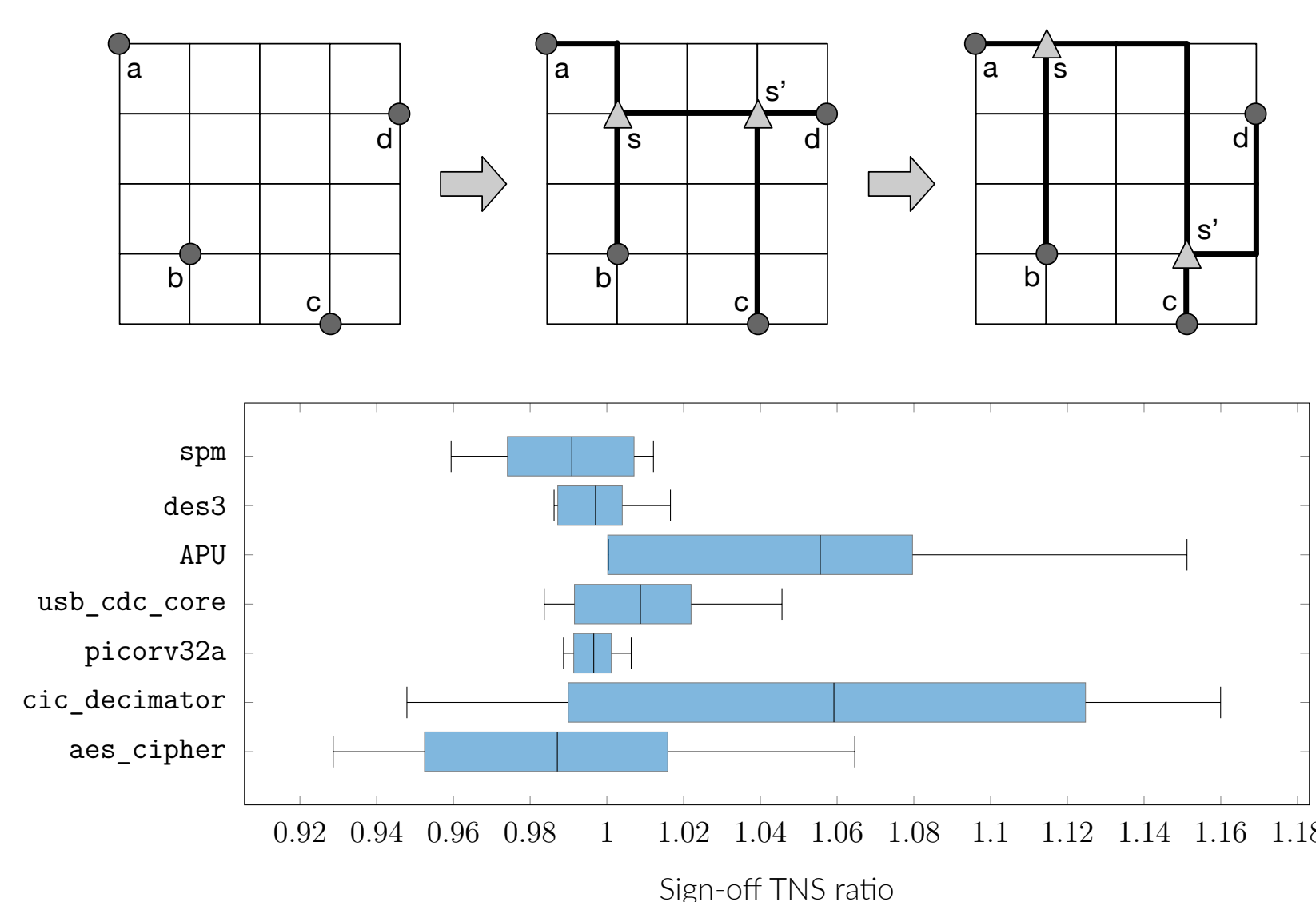
Background

Timing Closure

- Slack: $s_e = r_e - a_e$ for a timing path endpoint e , where r_e and a_e denote e 's required time and arrival time.
- Worst Negative Slack (WNS): $w(\cdot) = \min_e s_e$.
- Total Negative Slack (TNS): $t(\cdot) = \sum_e \{\min\{0, s_e\}\}$

Timing awareness has been extended to most phases of the physical design flow for the timing closure.

Timing Optimization via Steiner point Refinement

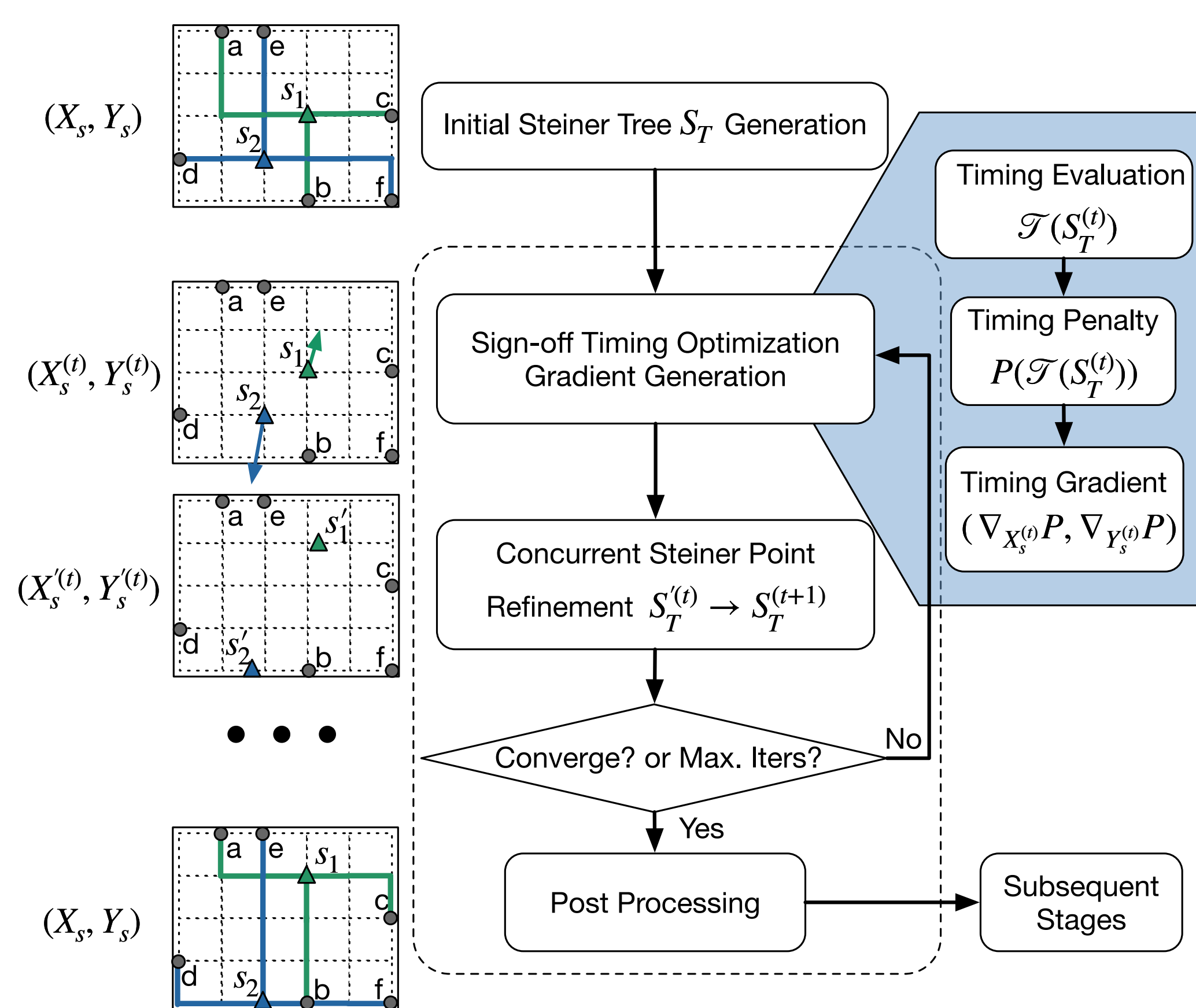


Highlights

- The sign-off timing performance could be significantly affected even by a random disturbance on Steiner point position.
- The impact of random moving is considerably unstable, and its average performance is slight.

Timing-driven Steiner point refinement Given an initial Steiner tree set $S_T = \{T^1, T^2, \dots, T^n\}$, $T^i = (V_c^i, V_s^i, E^i)$, where V_c^i is the set of cell nodes, V_s^i is the set of Steiner nodes and E^i means the edges connecting V_c^i and V_s^i of the i^{th} Steiner tree, our task is to refine the position (X_s, Y_s) of $V_s = \{V_s^i, 1 \leq i \leq n\}$ in the pre-routing stage to obtain better sign-off timing performance.

Overall Flow - TSteiner



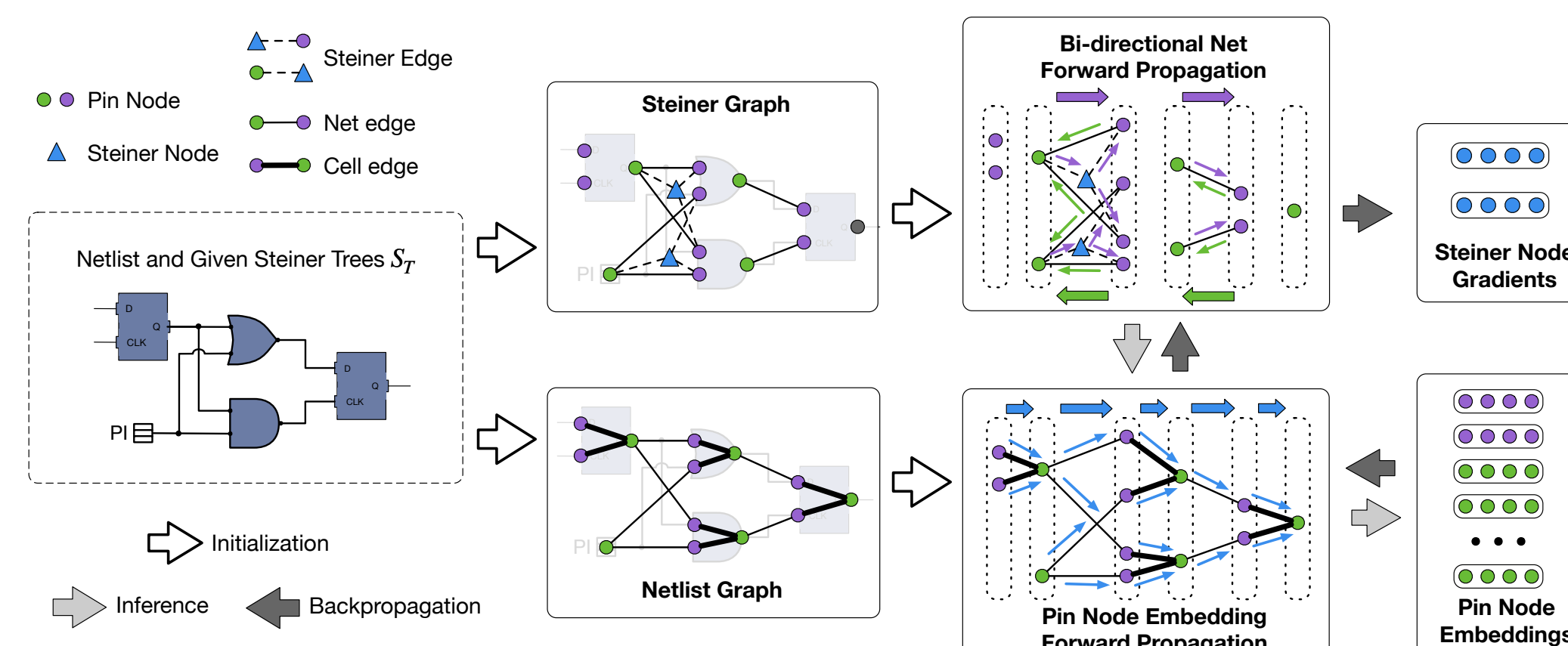
Highlights

- Sign-off timing optimization gradient $(\nabla_{X_s} P, \nabla_{Y_s} P)$ generation using timing evaluation model.
- Concurrent Steiner point refinement optimizes the Steiner points based on $(\nabla_{X_s} P, \nabla_{Y_s} P)$.

Evaluation Model

Sign-off Timing Evaluation Given a Steiner tree solution S_T , timing evaluation is to find an estimator \mathcal{T} to evaluate the sign-off timing metrics $\mathcal{T}(S_T)$, i.e., arrival time at each pin.

Evaluation Model



Highlights

- Node-, Net-, and Graph- Heterogenous.
- Bi-directional Net Forward Propagation and Pin Node Embedding Forward Propagation.

Timing Penalty

Timing penalty can be calculated as,

$$P(\mathcal{T}(S_T)) = \lambda_w w(\mathcal{T}(S_T)) + \lambda_t t(\mathcal{T}(S_T)), \quad (1)$$

Replace the maximum operation with the Log-Sum-Exp function LSE ,

$$LSE(x_1, x_2, \dots, x_n) = \gamma \log \left(\sum_{i=1}^n \exp \frac{x_i}{\gamma} \right), \quad (2)$$

the smoothed penalty function can be expressed as,

$$P_\gamma(\mathcal{T}(S_T)) = \lambda_w w_\gamma(\mathcal{T}(S_T)) + \lambda_t t_\gamma(\mathcal{T}(S_T)). \quad (3)$$

Steiner Point Optimization

Stochastic Optimization Algorithm $SO(X_s^{(t)}, \nabla_{X_s^{(t)}} P)$

$$m_x^{(t)} = (1 - \beta_1) \cdot \nabla_{X_s^{(t)}} P, \quad v_x^{(t)} = (1 - \beta_2) \cdot (\nabla_{X_s^{(t)}} P \odot \nabla_{X_s^{(t)}} P), \quad (4)$$

$$X_s^{(t)} = X_s^{(t-1)} - \theta \cdot \frac{m_x^{(t)}}{\sqrt{v_x^{(t)} + \epsilon}}$$

Adaptive Step Size Adaptive_Theta

- Obtain the initial timing gradient $(\nabla_{X_s} P, \nabla_{Y_s} P)$ w.r.t. the given Steiner point positions (X_s, Y_s) .
- Apply a small move:

$$X_s' = X_s + \alpha \nabla_{X_s} P, \quad Y_s' = Y_s + \alpha \nabla_{Y_s} P, \quad (5)$$
 where α is a hyper-parameter to control the scale of θ .
- Obtain the updated timing gradient $(\nabla_{X_s'} P, \nabla_{Y_s'} P)$.

The adaptive step size is then calculated as:

$$\theta = \frac{|(X_s, Y_s) - (X_s', Y_s')|_2}{|(\nabla_{X_s} P, \nabla_{Y_s} P) - (\nabla_{X_s'} P, \nabla_{Y_s'} P)|_2}. \quad (6)$$

Concurrent Steiner Point Refinement

Input: S_T : initial Steiner trees; \mathcal{T} : pre-trained timing prediction model; N : maximum optimization iterations; μ : converge ratio.

- $init_wns \leftarrow w(\mathcal{T}(S_T)); best_wns \leftarrow w(\mathcal{T}(S_T));$
- $init_tns \leftarrow t(\mathcal{T}(S_T)); best_tns \leftarrow t(\mathcal{T}(S_T));$
- $\theta \leftarrow Adaptive_Theta(S_T); t \leftarrow 0; S_T^{(0)} \leftarrow S_T; X_s^{(0)} \leftarrow X_s; Y_s^{(0)} \leftarrow Y_s;$
- Initialize the optimizer SO with θ ;
- repeat**
- $S_T^{(t)} \leftarrow SO(S_T^{(t)}, (\nabla_{X_s^{(t)}} P, \nabla_{Y_s^{(t)}} P));$
- $wns \leftarrow w(\mathcal{T}(S_T^{(t)})); tns \leftarrow t(\mathcal{T}(S_T^{(t)}));$
- if** $wns > best_wns$ or $tns > best_tns$ **then**
- $best_wns \leftarrow wns; best_tns \leftarrow tns; S_T^{(t+1)} \leftarrow S_T^{(t)};$
- else**
- $S_T^{(t+1)} \leftarrow S_T^{(t)};$
- end if**
- $t \leftarrow t + 1;$
- if** $t \geq N$ **then**
- break;**
- end if**
- until** $\frac{init_wns - best_wns}{init_wns} > \mu$ or $\frac{init_tns - best_tns}{init_tns} > \mu$
- return** $S_T^{(t)}$ (Resulting Steiner Trees)

Results

Table 1. Sign-off Timing prediction performance on two tasks, where 'arrival-all' and 'arrival-ends' represent the arrival time prediction on all pins and only endpoints, respectively.

Benchmark	chacha	cic_decimator	APU	des	jpeg_encoder	spm	Avg. Train
arrival-all	0.9882	0.9980	0.9950	0.9989	0.9959	0.9991	0.9959
arrival-ends	0.9979	0.9990	0.9977	0.9976	0.9936	0.9987	0.9974

Benchmark	aes_cipher	picorv32a	usb_cdc_core	des3	Avg. Test
arrival-all	0.9468	0.9401	0.9163	0.9087	0.9280
arrival-ends	0.9459	0.9498	0.7015	0.9510	0.8871

Table 2. Comparison with the routing flow without integrating TSteiner.

Benchmark	CUGR [1] + TritonRoute [2]					TSteiner + CUGR [1] + TritonRoute [2]						
	WNS (ns)	TNS (ns)	# Vios	WL(x10 ⁶)	# DRV	WNS (ns)	TNS (ns)	# Vios	WL(x10 ⁶)	# DRV		
aes_cipher	-11.246	-1516.9	512	984.971	109574	5	-8.38	-1434.2	504	984.527	109443	3
chacha	-48.538	-26259.1	1378	1,257,427	126600	2	-46.68	-25375.7	1372	1,258.011	126898	2
cic_decimator	-2.834	-169.981	72	16.466	5586	3	-2.724	-161.436	72	16.413	5593	3
picorv32a	-17.762	-441.607	67	727.216	109293	38	-17.686	-434.443	56	727.472	109311	37
usb_cdc_core	-5.914	-1365.2	347	49.351	12396	0	-5.823	-1343.1	346	49.117	12407	0
APU	-2.265	-33.713	25	101.179	23031	3	-2.221	-33.598	25	101.454	23101	3
des	-7.352	-405.427	341	682.828	115698	5	-3.987	-227.331	285	682.788	115599	5
jpeg_encoder	-74.342	-64909.2	1967	2,969,654	439126	1	-70.629	-60789.1	2007	2,973.304	439561	1
des3	-7.048	-1890	1512	2,680,848	372583	48	-5.668	-1879.6	1509	2,684.367	372768	49
spm	-0.817	-65.866	126	4.394	1553	2	-0.782	-63.846	126	4.399	1544	2
Average	1.000	1.000	1.000	1.0000	1.0000	1.0000	0.888	0.929	0.967	0.9999	1.0001	0.9549

Table 3. Runtime (s) breakdown

Benchmark	[1] + [2]		TSteiner + [1] + [2]	
	Total	[1]	Total	TSteiner
aes_cipher	539.847	16.781	523.066	22.222
chacha	480.123	19.795	460.328	17.830
cic_decimator	133.794	0.592	133.202	21.642
picorv32a	406.286	12.622	393.664	20.174
usb_cdc_core	54.660	1.247	53.413	0.529
APU	95.120	2.299	92.821	13.109
des	243.901	10.725	233.176	13.109
jpeg_encoder	893.485	61.433	832.052	33.563
des3	558.014	37.863	520.151	2.479
spm	11.848	0.307	11.541	0.279
Ratio Avg.	1.000	1.000	1.000	1.320

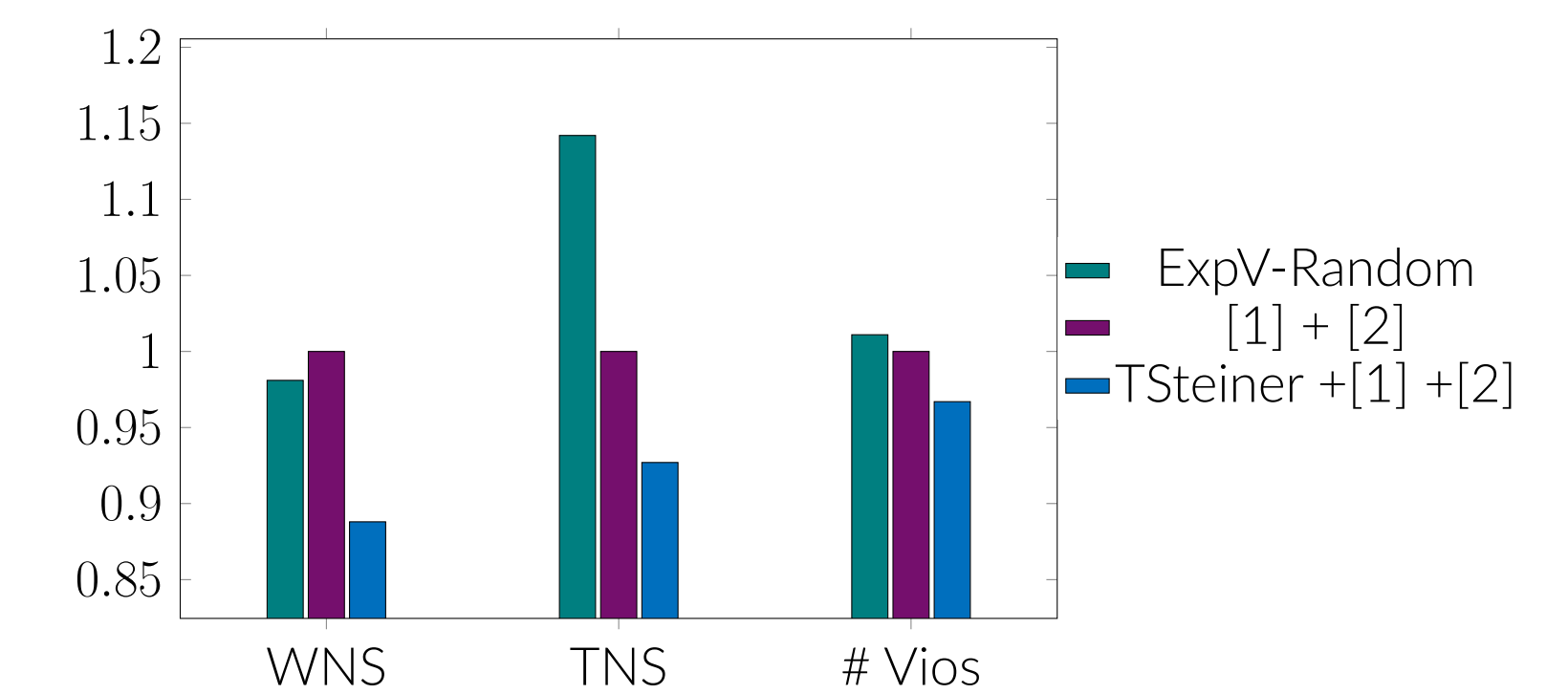


Figure 1. Sign-off timing metrics ratio comparison. 'ExpV-Random' represents the average expected value with 10-50 times random moves.

Highlights

- Our proposed timing evaluation model can accurately predict sign-off timing metrics.
- TSteiner brings **11.2%** and **7.1%** on average and up to **45.8%** and **43.9%** improvement for WNS and TNS, respectively.
- TSteiner brings only a little runtime overhead and comparable routing solution quality.

Conclusion & Future Directions

- This study has raised the importance of Steiner point refinement for timing closure and provides a novel solution for early-stage timing optimization.
- TSteiner can be extended to more physical stages since Steiner points exist not only in the pre-routing stage but also in routing solutions.

References

- J. Liu, C.-W. Pui, F. Wang, and E. F. Young, "CUGR: Detailed-routability-driven 3d global routing with probabilistic resource model," in Proc. DAC, pp. 1-6, 2020.
- A. B. Kahng, L. Wang, and B. Xu, "Tritonroute: The open-source detailed router," IEEE TCAD, vol. 40, no. 3, pp. 547-559, 2020.

